

# Performances improvement of eosin Y sensitized solar cells by modifying TiO<sub>2</sub> electrode with silane-coupling reagent

ZHOU YanFang<sup>1,2</sup>, LI XuePing<sup>1</sup>, ZHANG JingBo<sup>1</sup>, ZHOU XiaoWen<sup>1</sup> & LIN Yuan<sup>1†</sup>

<sup>1</sup> CAS Key Laboratory of Photochemistry, Institute of Chemistry, Chinese Academy of Sciences, Beijing 100190, China;

<sup>2</sup> Graduate University of Chinese Academy of Sciences, Beijing 100049, China

**Chemical fixing of xanthene dye (eosin Y) on the surface of TiO<sub>2</sub> electrode was carried out by modifying the electrode with silane-coupling reagent to obtain stable dye-sensitized TiO<sub>2</sub> electrode. Such silane modification can not only evidently enhance the stability of dye-sensitized TiO<sub>2</sub> electrode but also improve the energy conversion efficiency of the assembled cells by increasing short-circuit photocurrent ( $J_{SC}$ ) and open-circuit photovoltage ( $V_{OC}$ ). It was found that the improvements of cell performances differ depending on the composition of the electrolyte. The optimum cell of the cell performance was achieved in the electrolyte with 0.5 mol/L TBAI/0.05 mol/L I<sub>2</sub>/EC:PC(3:1 w/w), yielding  $J_{SC}$  of 4.69 mA·cm<sup>-2</sup>,  $V_{OC}$  of 0.595 V, fill factor (FF) of 0.64 and  $\eta$  of 1.78%. Different spectroscopic techniques including UV-Vis spectra, fluorescence spectra, EIS and dark current measurements were employed to derive reasonable analysis and explanations.**

silane-coupling reagent, dye-sensitized solar cells, eosin Y, organic dye, TiO<sub>2</sub> electrode, modification

As a novel renewable, clean photoelectric conversion system and potential alternative to the traditional photovoltaic devices, dye-sensitized solar cells (DSSCs) based on nanocrystalline porous TiO<sub>2</sub> thin films have attracted great attention and have been investigated intensively due to their high energy conversion efficiencies and low production costs<sup>[1,2]</sup>. In the simplest version, DSSCs consist of three components: dye-sensitized nanocrystalline TiO<sub>2</sub> photoanode, platinized counter electrode and electrolyte containing iodide(I<sup>-</sup>)/triiodide (I<sub>3</sub><sup>-</sup>) redox couple. The functions of these cells are based on the injection of electrons from photoexcited dye (D\*) to the conduction band of the nanocrystalline TiO<sub>2</sub>. The oxidized dye (D<sup>+</sup>) is regenerated by iodide (I<sup>-</sup>) and the reduction of produced triiodide (I<sub>3</sub><sup>-</sup>) in this reaction is achieved on the counter electrode. Whether the efficient operation of DSSCs could be maintained depends on both efficient electron injection and efficient dye regeneration. Therefore, the lowest unoccupied molecular

orbital (LUMO) energy level of dye must be amply higher than the conduction band edge minimum ( $E_{CB}$ ) of TiO<sub>2</sub> for efficient electron injection, and in the meantime, the potential of the redox couple (I<sup>-</sup>/I<sub>3</sub><sup>-</sup>) in the electrolyte ( $E_{redox}$ ) must be higher than the highest occupied molecular orbital (HOMO) energy level of dye for efficient dye regeneration, which is the key to keep the photocurrent production. The maximum photovoltage of DSSCs corresponds to the difference of the Fermi level ( $F_f$ ) of TiO<sub>2</sub> and the redox potential of the electrolyte.

In order to improve the photoelectric conversion properties of DSSCs, such as short-circuit photocurrent ( $J_{SC}$ ), many dye sensitizers have been investigated and employed in DSSCs. Especially, Rupolypyridyl complexes,

Received March 4, 2009; accepted May 24, 2009

doi: 10.1007/s11434-009-0440-8

†Corresponding author (email: linyuan@iccas.ac.cn)

Supported by the National Research Fund for Fundamental Key Project (Grant No. 2006CB202605), High-Tech Research and Development Program of China (Grant No. 2007AA05Z439) and National Natural Science Foundation of China (Grant No. 20873162)

such as cis-[Ru(dcbH<sub>2</sub>)<sub>2</sub>(NCS)<sub>2</sub>](N3), (Bu<sub>4</sub>N)<sub>2</sub>[Ru(dcbpy-H)<sub>2</sub>(NCS)<sub>2</sub>](N719) and Ru(NCS)<sub>3</sub>(tctpy)(black dye) have been intensively investigated. They still represent the most efficient sensitizers and have achieved highest energy conversion efficiency of 10%–11% in DSSCs so far<sup>[3]</sup>. But, metal-free organic dyes, such as xanthenes<sup>[4,5]</sup>, coumarines<sup>[6–9]</sup>, porphyrins<sup>[10,11]</sup> and indolines<sup>[12–14]</sup>, are also highly competitive candidates for use as sensitizers for DSSCs owing to their high molar excitation extinction coefficient, easy preparation, low cost and complicated structures. These dye structures all can provide COOH-based anchoring group for connecting the TiO<sub>2</sub> surface. Compared to Rupolypyridyl complexes, the above mentioned organic dyes, in most cases, have only one anchoring group, which should affect the fixation of dye on TiO<sub>2</sub> surface. A better way to solve this problem is the modification of TiO<sub>2</sub> electrode with silane-coupling reagent. Fujihira and Abe have fixed the sensitizers on the surface of TiO<sub>2</sub> by using silane-coupling reagents to overcome the unstableness of the metal-free organic dye-sensitized TiO<sub>2</sub><sup>[15,16]</sup>. As mentioned above, it is necessary that HOMO and LUMO energy levels of dye sensitizers should match well with the redox potential of the redox couple in the electrolyte and the conduction band edge minimum of the TiO<sub>2</sub>, respectively. Organic xanthene dye (eosin Y) can well satisfy these thermodynamic requirements and provide enough driving force for both electron injection and dye regeneration<sup>[17]</sup>. Although the device conversion efficiency based on eosin Y was still low<sup>[18–23]</sup>, we investigated the effect of silane modification on the performances of organic dye-based DSSCs. Maybe pathways were opened to utilize a variety of other sensitizers other than the established Ru complexes. Herein, we characterize the modification of TiO<sub>2</sub> electrode with silane-coupling reagent and the stability of these electrodes using different spectroscopic methods, and the photoelectric conversion properties of assembled DSSCs are investigated.

## 1 Experimental

### 1.1 Chemicals

TiO<sub>2</sub> powder was purchased from Dugussa (P25). Lithium iodide (LiI), iodine (I<sub>2</sub>), 3-methoxypropionitrile (MP), ethylene carbonate (EC) and propylene carbonate (PC) were purchased from Acros. *n*-butanol (C<sub>4</sub>H<sub>9</sub>OH), tetrabutyl titanate (Ti(OC<sub>4</sub>H<sub>9</sub>)<sub>4</sub>), acetic acid (HAc) and tetrabutylammonium iodide (TBAI) were purchased

from Beijing Chemical Company (analytic reagent grade).  $\gamma$ -Aminopropyltriethoxysilane (KH550), 3-glycidoxypropyltrimethoxysilane (KH560) (Diamond Advanced Material Of Chemical Inc.) and other chemicals were of analytic reagent grade and used as received without further purification.

### 1.2 The preparation of dye-sensitized TiO<sub>2</sub> electrodes

The preparation of the nanocrystalline TiO<sub>2</sub> colloid A is described as follows: A mixture of *n*-butanol solution (60 mL) and distilled water (3 mL) were added dropwise to a well stirred sample of *n*-butanol (40 mL) solution containing tetrabutyl titanate (10 mL) and acetic acid (4 mL). The solution was stirred for a while and then autoclaved at 180°C for 4h. In order to improve the cell performance, 5% by weight of P25 was added into colloids A, which resulted in colloid B. Colloid A was coated on cleaned conducting glass (fluorine-doped SnO<sub>2</sub>, 20 ohm/square) by using doctor-blade technique. Obtained TiO<sub>2</sub> thin film was dried at room temperature and then sintered at 450°C for 30 min. The second layer thin film was prepared by colloid B, and then heated at the same temperature for 30 min. Film thickness of the obtained electrode measured about 6  $\mu$ m.

For the modification of TiO<sub>2</sub> electrode, 5% (v:v) KH550 was stirred in 95% EtOH aqueous solution for 1 h at room temperature<sup>[16]</sup>. After stirring, TiO<sub>2</sub> electrode was dipped in the solution for different time, and then washed by EtOH for several times to remove the excess KH550 on the surface of TiO<sub>2</sub>. The as-prepared electrode will be referred to as KH550-TiO<sub>2</sub>. The KH550-TiO<sub>2</sub> electrodes were dye-coated by immersing them in 5 $\times$ 10<sup>-4</sup> mol/L dye solution of eosin Y in absolute ethanol for 12 h. Afterwards, the dye-sensitized electrodes were rinsed with absolute ethanol and dried in air.

### 1.3 Spectral measurements

X-ray photoelectron spectroscopy (XPS) analyses were made using an ESCALab220i-XL electron spectrometer from VG Scientific with 300 W Al *K* $\alpha$  radiation. All spectra were taken at a working pressure of about 3 $\times$ 10<sup>-9</sup> mbar. The binding energy was calibrated using the C1s line at 284.6 eV from adventitious carbon. Wide-scan spectra were recorded in the range of 0–1200 eV.

The surface treatments of the TiO<sub>2</sub> thin film were investigated by Fourier transformed infrared spectroscopy

(FTIR) to determine the presence of KH550 on the TiO<sub>2</sub> thin film. The spectra were obtained with transmittance mode using KBr pellets. All samples were detected on a Bruker Tensor 27 FTIR spectrometer (DLATGS detector) using signal averaged scans at a resolution of 4 cm<sup>-1</sup>. UV-Vis absorption spectra were measured on a Hitachi 3010 UV/Vis Spectrophotometer.

The steady state fluorescence spectra were recorded with a Hitachi F-4500 Spectrometer. Samples were contained in a square quartz cuvette (10 mm × 10 mm), and the detector was always at 90° to the exciting light beam. The exciting wavelength is 489 nm.

#### 1.4 Photoelectrochemical and electrochemical measurements

The two-electrode sandwich cells which consisted of a counter electrode (a Pt foil), a working electrode (a dye-sensitized TiO<sub>2</sub> electrode), and redox electrolytes containing triiodide and iodine were clamped firmly together. The photoelectrical properties of assembled cell were measured with a PAR potentiostat (model 273) under 100 mW · cm<sup>-2</sup> irradiation at room temperature. A 400 W xenon lamp with a 10 cm water filter was used as a light source, and the active cell area was 0.2 cm<sup>2</sup>.

Electrochemical impedance spectra (EIS) were measured by using Solartron 1255B frequency response analyzer and Solartron SI 1287 electrochemical interface system using a perturbation of ± 10 mV over the open circuit potential. The spectra were scanned in a frequency range of 1 MHz to 1 Hz at room temperature. All measurements were carried out under illumination of 100 mW · cm<sup>-2</sup>.

## 2 Results and discussion

### 2.1 Spectral characteristics of different TiO<sub>2</sub> thin film electrodes

The surface composition of two different TiO<sub>2</sub> thin film electrodes—pure TiO<sub>2</sub> and KH550-TiO<sub>2</sub> was studied by XPS measurements. From their XPS survey scan spectra shown in Figure 1, the XPS peaks of Ti 2s, Ti 2p and O1s can be only found for pure TiO<sub>2</sub> thin film (Figure 1(b)), but the additional peaks of N 1s, Si 2s and Si 2p were clearly observed for KH550-TiO<sub>2</sub> thin film (Figure 1(a)). This confirms the presence of KH550 on TiO<sub>2</sub> thin film and the coupling of KH550 with TiO<sub>2</sub> surface.

The FTIR spectral characteristics of the pure TiO<sub>2</sub> and KH550-TiO<sub>2</sub> thin films are shown in Figure 2. It was fo-

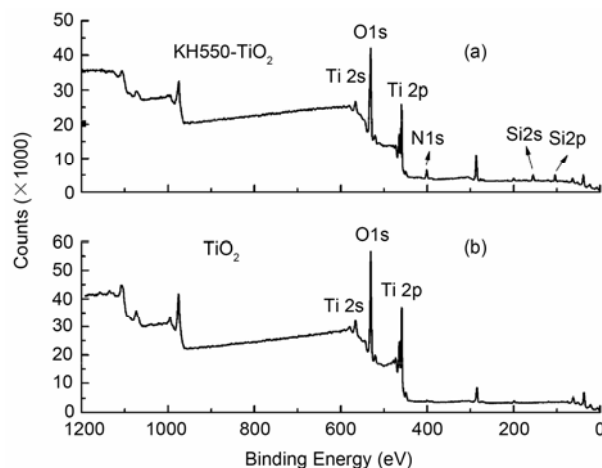


**Figure 1** XPS survey spectra of the pure TiO<sub>2</sub> and KH550-TiO<sub>2</sub> thin films.

und that the stretching vibration of —OH band at 3400 cm<sup>-1</sup> was obviously reduced and the δNH band at 1654 cm<sup>-1</sup> and Si—O—Ti band at 1124 cm<sup>-1</sup> clearly appeared on KH550-TiO<sub>2</sub> thin films, which further convinced the existence of KH550 on the surface of TiO<sub>2</sub> thin films and the coupling reaction between them.

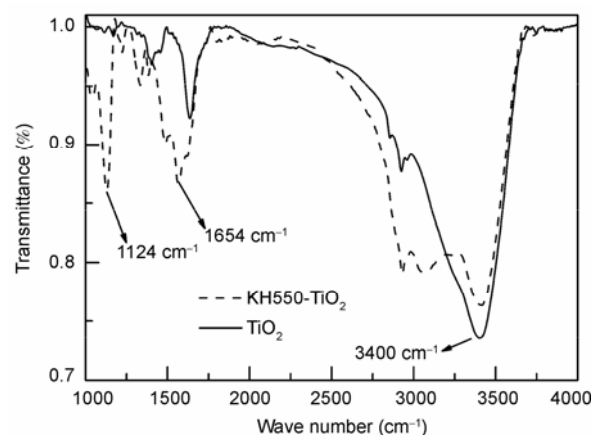


**Figure 2** FTIR spectra of the pure TiO<sub>2</sub> and KH550-TiO<sub>2</sub> thin films.

In order to confirm that the binding of eosin Y molecules on the surface of TiO<sub>2</sub> thin film is based on amino group, another silane-coupling reagent KH560 without amino group is employed for comparison. The TiO<sub>2</sub> thin film electrode modified with KH560 is referred to as KH560-TiO<sub>2</sub>. Figure 3 displays the UV-Vis spectra of the desorbed eosin Y using NaOH aqueous solution of 0.5M/L from different TiO<sub>2</sub> thin film electrodes. The quantity of adsorbed dye on different TiO<sub>2</sub> thin film electrodes follows the order of KH550-TiO<sub>2</sub> > pure TiO<sub>2</sub>

> KH560-TiO<sub>2</sub>. It reveals that there is strong chemical bonding of dye molecules on the TiO<sub>2</sub> thin film by utilizing dehydration of carboxyl group (–COOH) of eosin Y dye with amino group (–NH<sub>2</sub>) of the silane-coupling reagent (KH550) fixed on the surface of TiO<sub>2</sub> thin film<sup>[16]</sup>. Therefore, the TiO<sub>2</sub> thin film electrode modified with KH550 has greater ability of adsorbing dye and stronger strength of fixing dye on TiO<sub>2</sub> electrode than the other two electrodes: TiO<sub>2</sub> and KH560-TiO<sub>2</sub>. The reason why KH560-TiO<sub>2</sub> brought about the lowest dye adsorption is the absence of reaction group –NH<sub>2</sub> in its molecule structure.

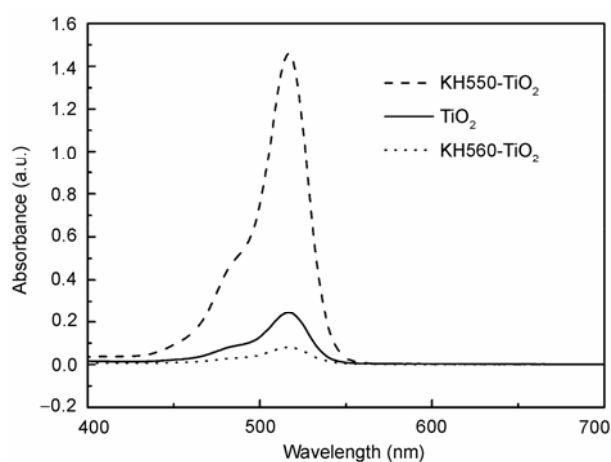


**Figure 3** UV-Vis spectra of the desorbed dye with 0.5 mol/L NaOH aqueous solution from different TiO<sub>2</sub> electrodes

The UV-Vis spectra of desorbed eosin Y dye from different TiO<sub>2</sub> electrodes before and after the photoelectrochemical measurements were further compared in Figure 4. The irradiation time was 3 h for all the samples. We find that eosin Y on pure TiO<sub>2</sub> electrode is easy to be desorbed in organic solvent presented in the electrolyte after measurements (curve b). This can be attributed to the unstable bonding between eosin Y and TiO<sub>2</sub>. But, only a little reduction on KH550-TiO<sub>2</sub> electrode was detected after the measurement (curve d), which again provides convincing evidence for stable bonding between eosin Y and KH550-TiO<sub>2</sub>. Such a slight decrease of desorbed eosin Y from KH550-TiO<sub>2</sub> electrode may be caused by that the silane-coupling reagent of KH550 does not completely react with all the OH groups on the TiO<sub>2</sub> thin film. We also observed that the eosin Y-sensitized TiO<sub>2</sub> electrode without modification discolored obviously after illumination while the color of eosin Y-sensitized KH550-TiO<sub>2</sub> electrode almost remained unchanged.

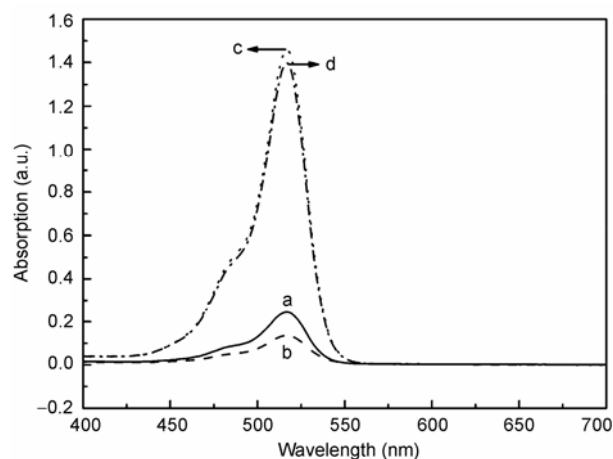
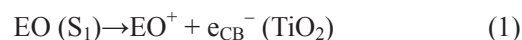


**Figure 4** UV-Vis spectra of desorbed eosin Y from different TiO<sub>2</sub> electrodes before and after the photoelectrochemical measurement (light intensity: 100 mW/cm<sup>2</sup>, active cell area: 0.2 cm<sup>2</sup>). a: TiO<sub>2</sub> electrode before measurements, b: TiO<sub>2</sub> electrode after measurements, c: KH550-TiO<sub>2</sub> electrode before measurements, d: KH550-TiO<sub>2</sub> electrode after measurements.

To investigate the property of interfacial electron transfer between eosin Y and TiO<sub>2</sub> thin film, fluorescence measurement was taken. After scraping from the corresponding thin film electrodes, pure TiO<sub>2</sub> and KH550-TiO<sub>2</sub> powders were added to ethanol solution of 1 × 10<sup>−5</sup> mol/L eosin Y, respectively. The PH value of obtained solution was kept at 7.0. From Figure 5, it can be observed that the addition of different TiO<sub>2</sub> powder (0.5 g/L) results in fluorescence quenching of eosin Y, which is attributed to the electron injection from singlet excited state of eosin Y to the conduction band of TiO<sub>2</sub> semiconductor (reaction (1))<sup>[17]</sup>.



where EO (S<sub>1</sub>) and EO<sup>+</sup> represent the singlet excitation

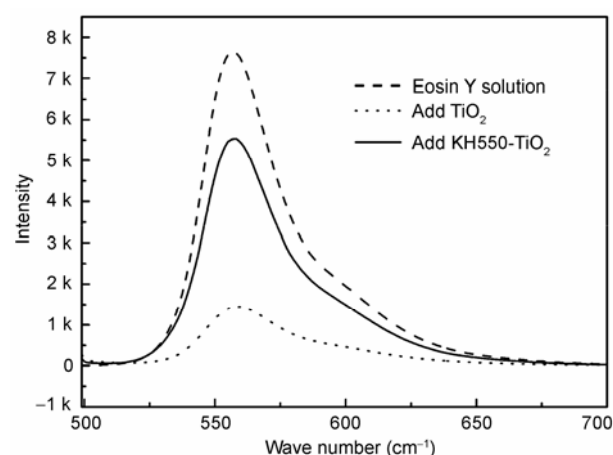


**Figure 5** Fluorescence emission spectra of 1 × 10<sup>−5</sup> mol/L eosin Y ethanol solution without and with different TiO<sub>2</sub> powders.

state of eosin Y and the oxidized eosin Y, respectively. The thermodynamic driving force for this electron transfer process is given by the difference between the redox potential of EO ( $S_1$ ) and the conduction band position of  $\text{TiO}_2$ . The value for the former is  $-1.2$  V (vs. NHE), while that for the latter is  $-0.5$  V (vs. NHE, PH = 7), indicating that there is sufficient driving force for this electron transfer reaction.

Furthermore, the fluorescence quenching of eosin Y is obviously weakened by KH550- $\text{TiO}_2$  compared with the unmodified  $\text{TiO}_2$ . This means that electron transfer from dye to  $\text{TiO}_2$  may be blocked because of the presence of KH550 on the surface of  $\text{TiO}_2$  electrode, resulting in weaker electron injection efficiency and lower  $J_{\text{SC}}$  of the cell. But the alkyl chain of KH550 on KH550- $\text{TiO}_2$  electrode can also prevent the recombination of  $e_{\text{CB}}^-(\text{TiO}_2)$  with  $\text{I}_3^-$  in the electrolyte, which is beneficial to the enhancement of  $V_{\text{OC}}$  of the cell. Therefore, we should find the equilibrium between these two opposite influence factors to improve the cell performance. This goal can be achieved by controlling the concentration of KH550 and the reaction time in preparing KH550- $\text{TiO}_2$  thin film electrode.

## 2.2 Dark current-voltage characteristics of DSSCs

In order to obtain larger  $V_{\text{OC}}$  and improve the efficiency of DSSCs, the dark current arising from the reduction of triiodide ( $\text{I}_3^-$ ) by the conduction band electrons at  $\text{TiO}_2$  thin film/electrolyte interface must be suppressed<sup>[23]</sup>. The surface modification of  $\text{TiO}_2$  electrode by using silane-coupling reagent is a more effective method for reducing the dark current of DSSCs<sup>[24,25]</sup>. In Figure 6,

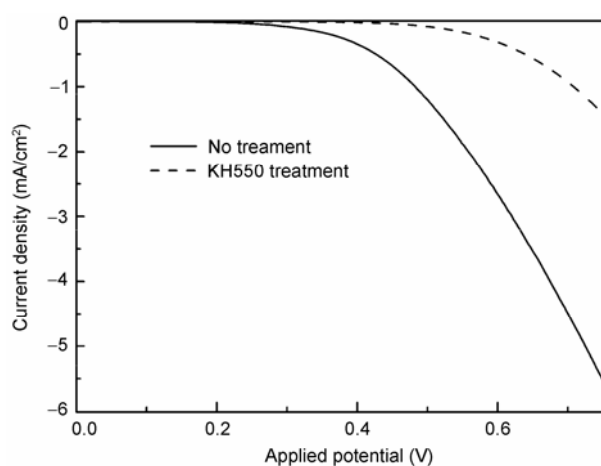


**Figure 6** Dark current-voltage characteristics of DSSCs with unmodified and KH550 modified  $\text{TiO}_2$  electrodes in the electrolyte A containing 0.5 M LiI, 0.05M  $\text{I}_2$  and 3-methoxypropionitrile.

the dark current-voltage curves of  $\text{TiO}_2$  electrodes with and without KH550 modification exhibit different characteristics. In comparison with unmodified  $\text{TiO}_2$  electrode, apparent decrease of the dark current and positive shift (nearly 100 mV) of its onset potential for KH550- $\text{TiO}_2$  electrode are clearly observed, indicating that the recombination of  $\text{I}_3^-$  and the conduction band electrons of  $\text{TiO}_2$  can be preserved by KH550 modification. The dark current onset potential is correlated with  $V_{\text{OC}}$ . The larger  $V_{\text{OC}}$  corresponds to larger dark current onset potential<sup>[22]</sup>. This can be proved by the following photovoltaic results (Figure 8).

The EIS measurement provides another useful evidence for suppressing the charge recombination of conduction band electrons of  $\text{TiO}_2$  and  $\text{I}_3^-$  in the electrolyte by silane modification. Figure 7 illustrates the Bode phase plots of DSSCs with different  $\text{TiO}_2$  electrodes at open circuit under  $100 \text{ mW} \cdot \text{cm}^{-2}$  illumination. In the spectra there are two characteristic frequency peaks: mid-frequency peak (in the 10–100Hz range) and high-frequency peak (in the kHz range) corresponding to the properties of photoinjected electrons in the  $\text{TiO}_2$  film and the charge transfer on the Pt counter electrode, respectively<sup>[26]</sup>. However, the low-frequency peak (in the mHz range) disappears. This condition often happens in the EIS measurement of DSSCs.

Obviously,  $\text{TiO}_2$  electrode modified with KH550 remarkably shifts the mid-frequency peak to lower frequencies and at the same time increases its amplitude compared with the unmodified  $\text{TiO}_2$  electrode. From the angular frequency ( $\omega_{\text{min}}$ ) at the mid-frequency peak, the

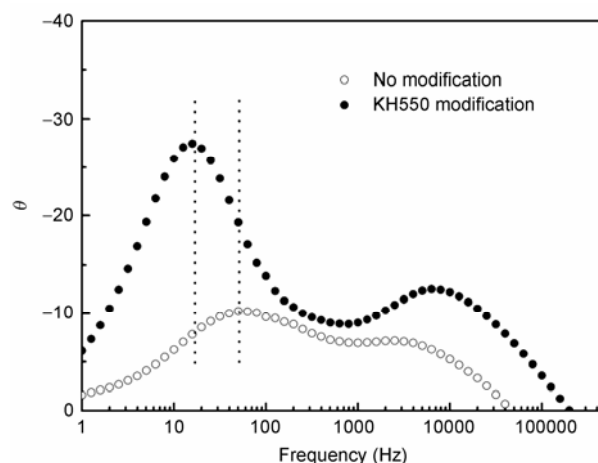


**Figure 7** Electrochemical impedance spectra of DSSCs with various  $\text{TiO}_2$  electrodes under open-circuit condition and illumination at  $100 \text{ mW} \cdot \text{cm}^{-2}$ , scanned from  $10^6$  to 1 Hz. Electrolyte: 0.5 mol/L LiI, 0.05 mol/L  $\text{I}_2$  and 3-methoxypropionitrile.

effective lifetime of electrons in TiO<sub>2</sub> conduction band ( $\tau_{\text{eff}}$ ) can be obtained according to the following relation (2)<sup>[26]</sup>:

$$\tau_{\text{eff}} \approx \frac{1}{\omega_{\text{min}}} \quad (2)$$

The lifetime is calculated to be 18.7 and 62.8 ms for DSSCs with unmodified and modified TiO<sub>2</sub> electrodes, respectively. This obvious increase of  $\tau_{\text{eff}}$  value also supports that the charge recombination of conduction band electrons of TiO<sub>2</sub> and I<sub>3</sub><sup>-</sup> can be suppressed by KH550 modification.

### 2.3 Photovoltaic characteristics of DSSCs

Figure 8 depicts the photocurrent density-voltage curves of DSSCs with unmodified and modified TiO<sub>2</sub> electrodes. The cells with KH550-TiO<sub>2</sub> or KH560-TiO<sub>2</sub> electrode exhibit 422mV, 416mV and evidently larger  $V_{\text{OC}}$  than those with unmodified TiO<sub>2</sub> electrode (318 mV). Moreover, the former has the same value (0.63) and larger FF than the latter (0.53). But,  $J_{\text{SC}}$  of the cell with KH560-TiO<sub>2</sub> electrode is prominently lower (0.68 mA · cm<sup>-2</sup>) than that with KH550-TiO<sub>2</sub> (3.44 mA · cm<sup>-2</sup>) or TiO<sub>2</sub> electrode (3.28 mA · cm<sup>-2</sup>). Therefore, the conversion efficiency of DSSCs with different TiO<sub>2</sub> electrodes decreased in the order of KH550-TiO<sub>2</sub> (0.91%) > TiO<sub>2</sub> (0.53%) > KH560-TiO<sub>2</sub> (0.18%). Obviously, the cell performance is improved considerably by using KH550-TiO<sub>2</sub> electrode. The larger  $V_{\text{OC}}$  is due to the inhibition of charge recombination of conduction band electrons of TiO<sub>2</sub> and I<sub>3</sub><sup>-</sup> by KH550 modification. The improvement of  $J_{\text{SC}}$  may be attributed to the increasing amount of adsorbed dye on KH550-TiO<sub>2</sub> electrode, thus benefiting the injection of electron to TiO<sub>2</sub> conduction band. These results well correspond to the preceding analyses and explanations of UV-Vis and fluorescence spectra.

**Table 1** Photovoltaic performances of DSSCs with KH550-TiO<sub>2</sub> electrode in different electrolytes

Electrolyte	$J_{\text{SC}}$ (mA · cm <sup>-2</sup> )	$V_{\text{OC}}$ (mV)	FF	$\eta$ (%)
A	3.44	422	0.63	0.91
B	3.82	560	0.64	1.36
C	4.69	595	0.64	1.78

A: 0.5 mol/L Lil + 0.05M I<sub>2</sub> + 3-Methoxypropionitrile; B: 0.5 mol/L KI + 0.05M I<sub>2</sub> + EC/PC(3:1 w/w); C: 0.5 mol/L TBAI + 0.05M I<sub>2</sub> + EC/PC(3:1 w/w).

Electrolyte usually plays an important part in determining the cell performances. By optimizing the electrolyte composition, cell performance with KH550-TiO<sub>2</sub>

electrode can be further improved. According to the literature<sup>[27,28]</sup>, cation species and solvents in the electrolytes have great impacts on the efficiency of DSSCs. The photovoltaic performances of cells with KH550-TiO<sub>2</sub> electrode in three electrolytes containing different iodides or organic solvents are listed in Table 1. It can be seen that the cell performances exhibit significant improvements by increasing the cation size of iodide or changing solvent from MP to EC/PC. Finally, comprehensively influenced by these two factors, the optimum cell performance was achieved in the electrolyte C, yielding  $J_{\text{SC}}$  of 4.69 mA · cm<sup>-2</sup>,  $V_{\text{OC}}$  of 595 mV,  $\eta$  of 1.78% and FF of 0.64.

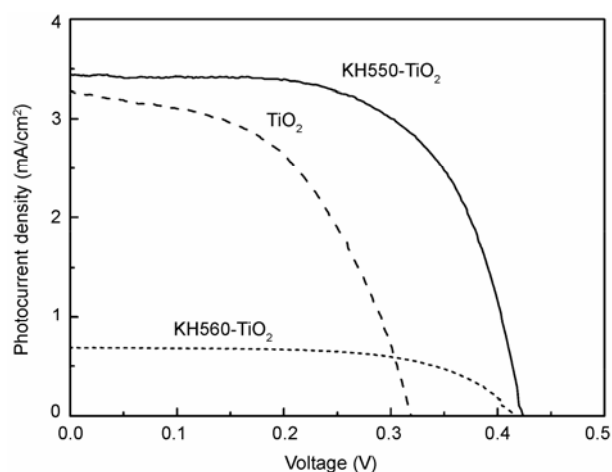


**Figure 8** Photocurrent-voltage characteristics of DSSCs with different TiO<sub>2</sub> electrodes in the electrolyte A containing 0.5 mol/L Lil, 0.05 mol/L I<sub>2</sub> and 3-methoxypropionitrile measured under illumination of 100 mW · cm<sup>-2</sup>

**Table 2** Cell performances of DSSCs based on TiO<sub>2</sub> electrodes with different silanization time

Silanization Time	$J_{\text{SC}}$ (mA · cm <sup>-2</sup> )	$V_{\text{OC}}$ (mV)	FF	$\eta$ (%)
0	3.43	555	0.64	1.23
3min	3.74	570	0.65	1.38
5min	4.69	595	0.64	1.78
15min	1.73	662	0.71	0.81

Electrolyte: 0.5 mol/L TBAI + 0.05 mol/L I<sub>2</sub> + EC/PC(3:1 w/w).

As mentioned above, the amount of KH550 on TiO<sub>2</sub> electrode reacts vigorously on the performances of solar cells. Herein, we control the amount of KH550 on TiO<sub>2</sub> by adjusting the silanization time of TiO<sub>2</sub> electrode. Table 2 lists the cell performances of DSSCs based on TiO<sub>2</sub> electrodes with different silanization time. As can be seen from the table, with the increase of treating time, the  $V_{\text{OC}}$  values show a tendency of increasing, due to the

inhibition of charge recombination by the presence of KH550. However, the  $J_{SC}$  values firstly increase to a maximum value in virtue of the increasing dye loading amount, and then tend to decrease under further silanization owing to the obstruction of electron injection. Finally, the highest performance is achieved when the silanization time is set at 5 min.

### 3 Conclusions

The performances of eosin Y dye-sensitized solar cells were improved through modifying nanocrystalline porous  $TiO_2$  electrode by silane-coupling reagent ( $\gamma$ -Aminopropyltriethoxysilane-KH550). The most prominent influences are as follows: 1) the decrease of dark current and the positive shift of the corresponding onset potential, resulting in the increase of  $V_{OC}$ ; 2) the increase of  $J_{SC}$  ascribed to the increased amount of adsorbed dye on modified  $TiO_2$  electrode surface; 3) the stability enhancement of eosin Y dye-sensitized  $TiO_2$  electrode in the electrolyte because of the strong chemical bonding

of dye molecules on the  $TiO_2$  electrode by using silane-coupling reagent KH550. These effects were well proved by different spectroscopic methods (UV-Vis spectra, fluorescence spectra, EIS) and dark current-voltage as well as photocurrent-voltage measurements. The cell performances can be further improved by optimizing the electrolyte composition, such as increasing the cation size of the iodide or changing solvent. In the electrolyte containing 0.5 mol/L TBAI, 0.05 M  $I_2$  and EC/PC (3:1 w/w), optimum cell performance was obtained, yielding  $J_{SC}$  of  $4.69 \text{ mA} \cdot \text{cm}^{-2}$ ,  $V_{OC}$  of 0.595 V, fill factor (FF) of 0.64 and  $\eta$  of 1.78%. Compared to the cell with unmodified  $TiO_2$  electrode, the energy conversion efficiency of the cell exhibited an apparent increase. Although the improved conversion efficiency is still lower compared with that of Ru complex-based DSSCs due to the nature of eosin Y, we believe that this method can be extended to other organic dyes, leading to the improvement of DSSCs performances based on organic dyes.

- Oregan B, Gratzel M. A Low-cost, high-efficiency solar-cell based on dye-sensitized colloidal  $TiO_2$  films. *Nature*, 1991, 353: 737—740.
- Hagfeldt A, Graetzel M. Light-induced redox reactions in nanocrystalline systems. *Chem Rev*, 1995, 95: 49—68
- Wang P, Zakeeruddin SM, Moser JE, et al. Stable new sensitizer with improved light harvesting for nanocrystalline dye-sensitized solar cells. *Adv Mater*, 2004, 16: 1806—1812
- El Mekkawi D, Abdel-Mottaleb MSA. The interaction and photostability of some xanthenes and selected azo sensitizing dyes with  $TiO_2$  nanoparticles. *Int J Photoenergy*, 2005, 7: 95—101
- Hara K, Horiguchi T, Kinoshita T, et al. Highly efficient photon-to-electron conversion with mercurochrome-sensitized nanoporous oxide semiconductor solar cells. *Sol Energy Mat Sol C*, 2000, 64: 115—134
- Hara K, Sato T, Katoh R, et al. Molecular design of coumarin dyes for efficient dye-sensitized solar cells. *J Phys Chem B*, 2003, 107: 597—606
- Hara K, Tachibana Y, Ohga Y, et al. Dye-sensitized nanocrystalline  $TiO_2$  solar cells based on novel coumarin dyes. *Sol Energy Mat Sol C*, 2003, 77: 89—103
- Wang ZS, Cui Y, Dan-Oh Y, et al. Thiophene-functionalized coumarin dye for efficient dye-sensitized solar cells: Electron lifetime improved by coadsorption of deoxycholic acid. *J Phys Chem C*, 2007, 111: 7224—7230
- Wang ZS, Cui Y, Hara K, et al. A high-light-harvesting-efficiency coumarin dye for stable dye-sensitized solar cells. *Adv Mater*, 2007, 19: 1138—1141
- Tokuhisa H, Hammond PT. Solid-state photovoltaic thin films using  $TiO_2$ , organic dyes, and layer-by-layer polyelectrolyte nanocomposites. *Adv Funct Mater*, 2003, 13: 831—839
- Nazeeruddin MK, Humphry-Baker R, Officer DL, et al. Application of metalloporphyrins in nanocrystalline dye-sensitized solar cells for conversion of sunlight into electricity. *Langmuir*, 2004, 20: 6514—6517
- Konno A, Kumara GRA, Kaneko S, et al. Solid-state solar cells sensitized with indoline dye. *Chem Lett*, 2007, 36: 716—717
- Horiuchi T, Miura H, Uchida S. Highly efficient metal-free organic dyes for dye-sensitized solar cells. *J Photoch Photobio A*, 2004, 164: 29—32
- Schmidt-Mende L, Bach U, Humphry-Baker R, et al. Organic dye for highly efficient solid-state dye-sensitized solar cells. *Adv Mater*, 2005, 17: 813—818
- Fujihira M. Photocell using covalently-bound dyes on semiconductor surfaces. *Nature*, 1976, 264: 349—350
- Abe R, Hara K, Sayama K, et al. Steady hydrogen evolution from water on eosin Y-fixed  $TiO_2$  photocatalyst using a silane-coupling reagent under visible light irradiation. *J Photoch Photobio A*, 2000, 137: 63—69
- Moser J, Graetzel M. Photosensitized electron injection in colloidal semiconductors. *J Am Chem Soc*, 1984, 106: 6557—6564
- Nguyen TV, Lee HC, Yang OB. The effect of pre-thermal treatment of  $TiO_2$  nano-particles on the performances of dye-sensitized solar cells. *Sol Energy Mat Sol C*, 2006, 90: 967—981
- Suri P, Mehra RM. Effect of electrolytes on the photovoltaic per-

- formance of a hybrid dye sensitized ZnO solar cell. *Sol Energy Mat Sol C*, 2007, 91: 518—524
- 20 Bando KK, Mitsuzuka Y, Sugino M, et al. Attachment of an organic dye on a TiO<sub>2</sub> substrate in supercritical CO<sub>2</sub>: Application to a solar cell. *Chem Lett*, 1999, 853—854
- 21 Kim S S, Yum J H, Sung Y E. Improved performance of a dye-sensitized solar cell using a TiO<sub>2</sub>/ZnO/eosin Y electrode. *Sol Energy Mat Sol C*, 2003, 79: 495—505.
- 22 Wang Z S, Sayama K, Sugihara H. Efficient eosin Y dye-sensitized solar cell containing Br<sup>-</sup>/Br<sub>3</sub><sup>-</sup> electrolyte. *J Phys Chem B*, 2005, 109: 22449—22455
- 23 Kazuhiro Sayama, Maki Sugino, Hideki Sugihara, et al. Photosensitization of porous TiO<sub>2</sub> semiconductor electrode with xanthenes. *Chem Lett*, 1998: 753—754
- 24 Gregg B A, Pichot F, Ferrere S, et al. Interfacial recombination processes in dye-sensitized solar cells and methods to passivate the interfaces. *J Phys Chem B*, 2001, 105: 1422—1429
- 25 Spivack J, Siclovan T, Gasaway S, et al. Improved efficiency of dye sensitized solar cells by treatment of the dyed titania electrode with alkyl(trialkoxysilanes). *Sol Energy Mat Sol C*, 2006, 90: 1296—1307
- 26 Kern R, Sastrawan R, Ferber J, et al. Modeling and interpretation of electrical impedance spectra of dye solar cells operated under open-circuit conditions. *Electrochim Acta*, 2002, 47: 4213—4225
- 27 Argazzi R, Bignozzi C A, Yang M, et al. Solvatochromic dye sensitized nanocrystalline solar cells. *Nano Lett*, 2002, 2: 625—628
- 28 Pollard JA, Zhang D S, Downing J A, et al. Solvent effects on interfacial electron transfer from Ru(4,4'-dicarboxylic acid-2,2'-bipyridine)(2)(NCS)(2) to nanoparticulate TiO<sub>2</sub>: Spectroscopy and solar photoconversion. *J Phys Chem A*, 2005, 109: 11443—11452